Journal of Physics: Conference Series **161** (2009) 012037 doi:10.1088/1742-6596/161/1/012037

The Casimir effect: from quantum to critical fluctuations

Andrea Gambassi

Max-Planck-Institut für Metallforschung, Heisenbergstr. 3, D-70569 Stuttgart, Germany and Institut für Theoretische und Angewandte Physik, Universität Stuttgart, Pfaffenwaldring 57, D-70569 Stuttgart, Germany.

E-mail: gambassi@mf.mpg.de

Abstract. The Casimir effect in quantum electrodynamics (QED) is perhaps the best-known example of fluctuation-induced long-ranged force acting on objects (conducting plates) immersed in a fluctuating medium (quantum electromagnetic field in vacuum). A similar effect emerges in statistical physics, where the force acting, e.g., on colloidal particles immersed in a binary liquid mixture is affected by the classical thermal fluctuations occurring in the surrounding medium. The resulting Casimir-like force acquires universal features upon approaching a critical point of the medium and becomes long-ranged at criticality. In turn, this universality allows one to investigate theoretically the temperature dependence of the force via representative models and to stringently test the corresponding predictions in experiments. In contrast to QED, the Casimir force resulting from critical fluctuations can be easily tuned with respect to strength and sign by surface treatments and temperature control. We present some recent advances in the theoretical study of the universal properties of the critical Casimir force arising in thin films. The corresponding predictions compare very well with the experimental results obtained for wetting layers of various fluids. We discuss how the Casimir force between a colloidal particle and a planar wall immersed in a binary liquid mixture has been measured with femto-Newton accuracy, comparing these experimental results with the corresponding theoretical predictions.

1. Introduction

This contribution focuses on the Casimir effect which arises when one confines fluctuations of a different nature compared to those originally considered by Casimir in his pioneering work [1]. Indeed we shall be concerned here with the fluctuations of thermal origin which occur close to a second-order phase transition point (*critical point*). The resulting *critical* Casimir effect is apparently less widely known than the corresponding one within quantum electrodynamics (QED). Nonetheless, the associated femto-Newton forces at the sub-micrometer scale can be put to work in soft matter systems and their high degree of tunability might even be exploited for concrete applications in colloidal suspensions. However, before focusing on the Casimir effect due to critical fluctuations we first discuss in subsec. 2.1 the effect within QED, following in spirit the original derivation by Casimir [1]. In subsec. 2.2 we then explain how this effect arises in statistical physics upon approaching a critical point, highlighting the analogies and differences between the two. In sec. 3 we present an overview of the available theoretical predictions which are relevant for the qualitative and quantitative interpretation of the experimental results. A short summary, with perspectives and applications is presented in sec. 4.

2. The Casimir effect

2.1. The effect in Quantum Electrodynamics

The Casimir effect is named after Hendrik Casimir who discovered, 60 years ago, that – quite surprisingly – two parallel, perfectly conducting and uncharged metallic plates in vacuum *attract* each other due to the *quantum fluctuations* of the electromagnetic fields, even at zero temperature $T = 0$ [1]. Indeed the plates (assumed to be perfectly conducting) effectively impose boundary conditions (BCs) on the electromagnetic fields so that, more specifically, $\mathbf{E}_{\parallel}$, $\mathbf{B}_{\perp} = 0$ where $\mathbf{E}_{\parallel}$ and $\mathbf{B}_{\perp}$ are the components of the electric $\mathbf{E}$ and magnetic $\mathbf{B}$ fields which are parallel and transverse to the surfaces of the plates. As a result of these boundary conditions, the *fluctuation modes* of the fields in the space within the two plates are allowed to have only a specific set of L-dependent wave-vectors, where L is the separation between the parallel plates. For example, in the case of Dirichlet BCs, the component $k_{\perp}$ of the wave-vector $\mathbf{k}$ perpendicular to the plates assumes only the quantized values $k_{\perp} = \pi n/L$ with $n = 1, 2, \ldots$. Roughly speaking, the "unbalance" between the pressure exerted by the allowed modes within the plates and the one exerted by the modes outside them is at the origin of the Casimir effect. This statement can be made quantitative by calculating the size-dependent energy $\mathcal{E}(L)$ of the fluctuation modes of the electromagnetic fields which are allowed in the portion of the vacuum within the plates. According to QED, this is given by

$$\mathcal{E}(L) = \sum_{\text{modes}} \frac{1}{2}\hbar c|\mathbf{k}_{\text{modes}}|\,, \tag{1}$$

where $\mathbf{k}_{\text{modes}}$ are the corresponding wave-vectors and c is the speed of light. For perfectly conducting plates of large transverse area S, the expansion of $\mathcal{E}(L)$ in decreasing powers of L takes the form (in three spatial dimensions)

$$\mathcal{E}(L) = \mathcal{E}_{\text{bulk}} + \mathcal{E}_{\text{surf}}^{(1+2)} + S\frac{\hbar c}{L^3}\left[-\frac{\pi^2}{1440} + O((\kappa L)^{-2})\right], \tag{2}$$

where $\mathcal{E}_{\text{bulk}} \propto SL^1$ is the energy associated to the electromagnetic field of the vacuum in the absence of the plates and within a volume $S \times L$; $\mathcal{E}_{\text{surf}}^{(1+2)} = \mathcal{E}_{\text{surf}}^{(1)} + \mathcal{E}_{\text{surf}}^{(2)} \propto SL^0$ is the sum of the energies $\mathcal{E}_{\text{surf}}^{(i)}$ associated to the introduction of each single plate, *separately*, in the vacuum; The next term in the expansion (2), i.e.,

$$\mathcal{E}_{\text{Cas}}(L) \equiv -\frac{\pi^2}{1440}\,S\frac{\hbar c}{L^3}\,, \tag{3}$$

is proportional to SL^{-3} and represents the *interaction energy* between the two plates which is due to their *simultaneous* presence in space. This is the Casimir term we are interested in and which is responsible for the celebrated Casimir force. Further terms in the expansion are of order $O((\kappa L)^{-2})$ compared to $\mathcal{E}_{\text{Cas}}$, where κ is a material-dependent parameter which describes the deviations of the plates from the perfectly conducting behavior due to the *finite* conductivity of the metal. In the expansion (2) the first term $\mathcal{E}_{\text{bulk}}$ is a property of the vacuum, the second one ($\mathcal{E}_{\text{surf}}^{(1+2)}$) depends on the material properties of the plates, whereas the third one, $\mathcal{E}_{\text{Cas}}$ in eq. (3), is *universal* in that it does not depend on the specific material which the plates are made of, but only on geometrical properties (S and L) and on fundamental constants ($\hbar c$). The relevance of higher-order terms in the expansion (2) depends on the material parameter κ.

The Casimir term, the third of the the expansion of the vacuum energy $\mathcal{E}(L)$ in decreasing powers of L, actually gives rise to a measurable effect: a small displacement δL of one of the two plates results in a change $\delta\mathcal{E}(L)$ in the energy of the fields within the plates and therefore

in a force $F_{\rm in}(L) = -\delta\mathcal{E}/\delta L$ (pushing on the inner surface of each single plate). Focusing on one of the two plates, the contribution to the force $F_{\rm in}(L)$ due to the change of $\mathcal{E}_{\rm bulk}$ in $\mathcal{E}(L)$, i.e., $F_{\rm bulk} \equiv -\delta\mathcal{E}_{\rm bulk}/\delta L$, is actually canceled out by the force $F_{\rm out} = F_{\rm in}(L=\infty) = F_{\rm bulk}$ acting from the other side of the plate and due to the fluctuation modes in the corresponding half-space outside the plate. $\mathcal{E}_{\rm surf}$ does not change upon changing L so that the total force $F(L) = F_{\rm in}(L) - F_{\rm out}$ acting on each single plate is due only to the change in the Casimir energy:

$$\frac{F(L)}{S} = -\frac{\pi^2}{480}\frac{\hbar c}{L^4} \quad \text{for} \quad L \gg \kappa^{-1}\,. \tag{4}$$

The universal behavior encoded in this equation can only be detected at separations L between the plates which are much larger than the length scale κ^{-1}, being material-specific properties relevant at smaller distances. In particular, κ is related to the typical wave-vector at which the plates are no longer effective in imposing the boundary conditions on the fields. As a rough estimate, this scale is set by the plasma frequency ω_p of the metal (more detailed calculations support this argument [2]), i.e., $c\kappa \simeq \omega_p$, where $\omega_p \simeq 3\cdot 10^{15}$Hz for copper, yielding $\kappa^{-1} \simeq 0.3\mu$m. Attempts to verify experimentally eq. (4) started already in 1958 [3] but the first sound experimental confirmation came only 40 years later within the range of separations $0.5\mu\text{m} \lesssim L \lesssim 6\mu\text{m}$ [2, 4]. Apart from the relevance of this effect for possible technological applications in micro- and nano-electromechanical systems (MEMS and NEMS, respectively), in which the associated force is responsible for *stiction*, its precise measurement could provide a test of the validity of some fundamental laws down to the nano-meter scale, see, e.g., ref. [5].

2.2. The effect in Statistical Physics

Thirty years after the seminal paper by Casimir, M. E. Fisher and P. -G. de Gennes published a note "On the phenomena at the walls in a critical binary mixture" [6] in which it was shown that Casimir-like effects (i.e., *fluctuation-induced forces*) arise also in statistical physics if a medium in which fluctuations of a certain nature take place is spatially confined [7]. In order to understand how these effects arise and what their relation is with the Casimir effect described in subsec. 2.1, we briefly recall here some basic facts about binary mixtures, their critical point and the effect of confinement. The schematic phase diagram of a liquid binary mixture in the bulk is depicted in fig. 1. At constant pressure, the relevant thermodynamic variables are the temperature T and the mass fraction c_A of one of the two components in the mixture. For a certain concentration c_A, the two components of the mixture are mixed at low temperatures and the resulting liquid solution looks homogeneous in a test tube (schematically represented on the left of the phase diagram). Upon increasing the temperature, however, the liquid demixes into an A- and a B-rich solution and becomes inhomogeneous in the test tube (represented on the right), where the two solutions are typically separated by an interface. The transition between the mixed and the demixed phase occurs at the solid first-order transition line. At the lowest point (CP) of this line the transition becomes critical, i.e., second-order. This point is referred to as the (lower) *critical point*. The mixed and demixed phases can be distinguished by monitoring the so-called *order parameter* of the transition, which can be identified with the deviation $\delta c_A(\mathbf{x}) \equiv c_A(\mathbf{x}) - c_A$ of the *local* concentration $c_A(\mathbf{x})$ of, say, component A from its average value in the mixture. Indeed, the thermal average $\langle \delta c_A(\mathbf{x})\rangle$ of the order parameter is homogeneous in the mixed phase, whereas it assumes two different values in the A-rich and B-rich solution which coexist in the demixed phase. The order parameter is characterized by a spatial correlation length ξ, so that, within each single phase, $\langle \delta c_A(\mathbf{x})\delta c_A(\mathbf{x}')\rangle - \langle \delta c_A(\mathbf{x})\rangle\langle \delta c_A(\mathbf{x}')\rangle \propto \exp\{-|\mathbf{x}-\mathbf{x}'|/\xi\}$, where ξ depends on T and c_A. Upon crossing the first-order transition line, the correlation length stays finite, whereas it diverges upon approaching the critical point. The physical behavior of the system at the scale set by ξ is actually determined by the fluctuations of the order parameter, which becomes the relevant physical quantity for the description of the system. In terms of it, one can

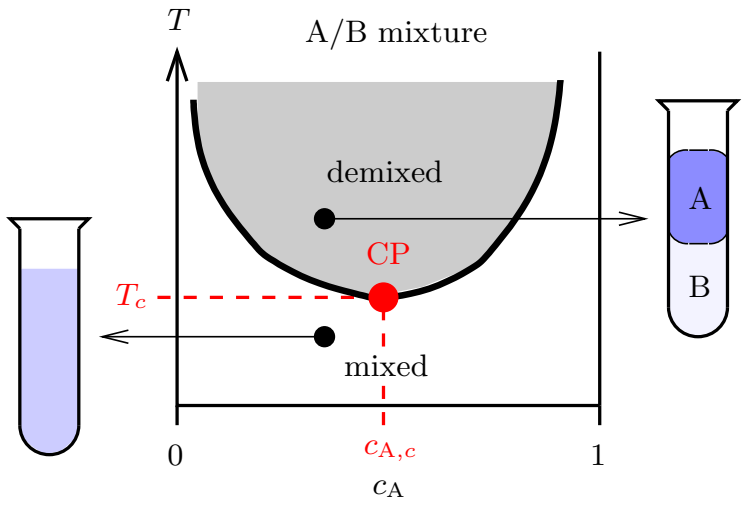

Figure 1. Schematic phase diagram of a binary liquid mixture with a lower critical point (CP). The schematic side views of a test tube filled with the binary liquid mixture in the mixed and in the demixed phase are shown on the left and on the right of the diagram, respectively.

express the effective free energy $\mathcal{F}$ of the system and determine its thermodynamic properties upon approaching the transition.

In order to understand the consequences of confining such a binary liquid mixture, we have first to consider the result of inserting a single plate (made up of, say, glass) into the mixture. In general one expects the plate to show preferential adsorption for one of the two components of the mixture, say A, due to quantitative differences in the interactions between each of them and the molecules of the plate. Accordingly, a plate in the mixture induces a local increase of the average order parameter $\langle \delta c_A(\mathbf{x}) \rangle$ close to it. Upon increasing the correlation length ξ (i.e., getting closer to the critical point), the plate effectively imposes boundary conditions on the order parameter [8, 9].

Table 1. Analogies and differences between the Casimir effect in (zero-temperature) QED and in Statistical Physics (see also footnote 1).

	QED	Stat. Phys
fluctuating quantity:	**E**, **B**	order parameter ϕ
excitation:	Quantum $\hbar c$ $(T = 0)$	Thermal(classical) $k_B T$ $(\hbar = 0)$
range of fluct.:	∞	finite: ξ $\xi \nearrow \infty$ close to CP
	$\Downarrow$	$\Downarrow$
	Confinement	
	$\Downarrow$	$\Downarrow$
	long-ranged force	range: ξ long-ranged at CP

Now that we have recalled how to describe the binary mixture in terms of a fluctuating order parameter (generically refereed to as ϕ in what follows) and the effects of inserted plates in terms of boundary conditions, it is easy to understand in which sense a Casimir-like interaction arises in these instances. Indeed (see table 1), the Casimir effect in QED emerges because there are some quantities (the fields **E** and **B**) which "fluctuate" in space and time due to the quantum nature of the "medium" (actually the vacuum) in which their fluctuations take place. Accordingly, the relevant scale of the phenomenon is set by $\hbar c$ at zero temperature. The two-point correlation function of the fluctuations of these quantities are characterized by an algebraic decay in space, i.e., the associated range is infinite (due to the vanishing mass $m_\gamma = 0$ of the photon). When the spectrum of these fluctuations gets modified by external bodies (metallic plates) which impose boundary conditions on the fluctuating fields, the associated energy $\mathcal{E}$ becomes a function of the position of these boundaries and as a result an effective long-ranged Casimir force arises on them. In statistical physics, close to a critical point, the relevant fluctuating quantity is the order parameter ϕ of the phase transition ($\phi(\mathbf{x}) = \delta c_A(\mathbf{x})$ in the case of the binary mixture) and its fluctuations are of thermal nature and due to the coupling between the system and the thermal bath at temperature T. Accordingly, the relevant scale of the phenomenon is $k_\mathrm{B}T$ and the fluctuations are of classical nature (i.e., $\hbar$ plays no role). The range of these fluctuations is given by ξ and therefore is *finite* but tunable upon approaching the critical point. As in the case of QED, external bodies impose boundary conditions on the order parameter ϕ and therefore they affect the spectrum of its allowed fluctuations and the associated effective free energy $\mathcal{F}$ depends on the positions of these bodies. As a result, a force is expected to act on them, with a range set by the correlation length ξ. In table 1 we summarize analogies and differences between the Casimir effect occurring in QED and in statistical physics[1]. Even though we have been referring to the case of a binary liquid mixture, the line of argument presented above extends to critical phenomena in general. Indeed, consider a medium close to its critical point and confined between two parallel plates at a distance L (film geometry). The medium might be, e.g., pure ^{4}He or a ^{3}He-^{4}He mixture close to the superfluid transition, a binary liquid mixture, a Bose gas close to the Bose-Einstein condensation, liquid crystals etc. If the correlation length ξ of the fluctuations of the order parameter and the thickness L of the film are much larger than the microscopic length scale ℓ_micr (set, say, by the molecular scale of the system), the *free energy* $\mathcal{F}$ of the confined medium can be decomposed in decreasing powers of L for a fixed value of L/ξ and large transverse area S, in analogy to eq. (2) [10, 11]

$$\mathcal{F}(T, L) = \mathcal{F}_\mathrm{bulk} + \mathcal{F}_\mathrm{surf}^{(1+2)} + S\frac{k_\mathrm{B}T}{L^2}\Theta_\parallel(L/\xi) + \mathrm{corr}. \tag{5}$$

We have assumed here that the only relevant thermodynamic variable is the temperature T, which determines the correlation length $\xi \sim \xi_0|(T - T_c)/T_c|^{-\nu}$ where ξ_0 is a system-specific quantity and ν a *universal* exponent, in the sense specified below. Possible additional thermodynamic variables, such as the concentration c_A of the binary mixture, are assumed to be tuned to their critical values, i.e., $c_A = c_{A,c}$ with reference to fig. 1. In the expansion (5) the first term $\mathcal{F}_\mathrm{bulk}$ is the free energy of the *bulk* medium in a volume $S \times L$, i.e., $\mathcal{F}_\mathrm{bulk} \propto SL$, the second one ($\mathcal{F}_\mathrm{surf}^{(1+2)}$) represents the sums of the free energy costs $\mathcal{F}_\mathrm{surf}^{(i)} \propto S$ for the separate introduction of the two walls in the system, i.e., $\mathcal{F}_\mathrm{surf}^{(1+2)} = \mathcal{F}_\mathrm{surf}^{(1)} + \mathcal{F}_\mathrm{surf}^{(2)}$. The third term represents, as in eq. (2), the *interaction (free)energy* between the two walls. Compared to the analogous term in the case of QED we note, as expected, that $k_\mathrm{B}T$ replaces $\hbar c$ in providing the scale of the phenomenon [2] and that the interaction between the two walls is no longer long-ranged but its

[1] In some cases the correspondence illustrated in table 1 goes beyond the mere analogy. Indeed, for the simplest geometrical settings, such as film geometry, there is a mapping between the Casimir effect in QED in d spatial dimensions and the effect at the critical point of the so-called Gaussian model in $d + 1$ dimensions.

[2] Due to the different engineering dimensions of $[\hbar c]$ = energy × length and $[k_\mathrm{B}T]$ = energy, and taking into

range is set by ξ via the dependence on L/ξ of the scaling function $\Theta_\parallel$([3]). This dependence can be understood as follows: the perturbation that the wall induces on the order parameter extends within a distance $\sim \xi$ far from it, so that the two walls can interact with each other only at separations $L \lesssim \xi$ whereas the interaction energy vanishes for $L \gg \xi$, so that $\Theta_\parallel(x \to \infty) = 0$.

The scaling function $\Theta_\parallel$ is *universal* (as the analogous term $\mathcal{E}_{\rm Cas}$ (3) in eq. (2)) in the sense that it depends only on some gross features of:

(a) the system in the bulk, such as the range and symmetries of the interaction and the kind of order parameter which describes the phase transitions,

(b) the surfaces which provide the confinement, such as the possible symmetries of the bulk system which they break, e.g., by favoring certain values of the order parameter at the boundaries. These preferences eventually translate into effective boundary conditions for the order parameter [8, 9]. In addition, $\Theta_\parallel$ depends on the shape of the boundaries, as we shall see below.

The general features at points (a) and (b) define the so-called *bulk* and *surface universality classes* of the confined system, respectively. This universality is typical of critical phenomena and allows one to investigate universal properties such as ν and $\Theta_\parallel$ by means of suitable representative models belonging to the same bulk and surface universality classes of the actual system one is interested in and which lend themselves for a simpler theoretical analysis. Analogously to what happens in QED, a small change δL of the distance between the confining surfaces leads to a change $\delta\mathcal{F}$ in the free energy and therefore to a force $-\delta\mathcal{F}/\delta L$ acting on the displaced wall. The L-independent contribution to this force due to $\mathcal{F}_{\rm bulk}$ in eq. (5) is counterbalanced by the same contribution acting from outside the walls when they are immersed in the critical medium, so that the net force $F(L,T)$ is given by (see eq. (5))

$$\frac{F(T,L)}{S} = \frac{k_{\rm B}T}{L^3}\vartheta_\parallel(L/\xi) \quad \text{for} \quad L,\, \xi \gg \ell_{\rm micr}, \tag{6}$$

where $\vartheta_\parallel(u) = -2\Theta_\parallel(u) + u\Theta'_\parallel(u)$ and it shares with $\Theta(u)$ the properties of universality. The universal scaling function $\vartheta_\parallel$ can be conveniently determined from the analysis of suitable representative models, either via field-theoretical methods or Monte Carlo simulations. In turn, the resulting predictions can be very stringently compared with the experimental determination of $\vartheta_\parallel$.

2.3. The force of quantum and critical fluctuations

In the preceding two sections we have briefly reviewed the origin of the Casimir effects due to quantum and critical fluctuations, highlighting the analogies and differences between them and the corresponding scaling and universal properties. In view of possible experimental investigations, however, it is important to estimate the expected magnitude of these effects. Assuming (quite unrealistically, indeed) that one is able to realize a system of two parallel plates of area $S = 1\,\mathrm{cm}^2$ at a distance $L = 1\,\mu\mathrm{m}$, the zero-temperature Casimir force resulting from quantum fluctuations is roughly estimated as $\sim S \times \hbar c/L^4 \simeq 6 \cdot 10^{-7}\,\mathrm{N}$, whereas the force due to critical fluctuations possibly occurring at room temperature ($T \simeq 300\,\mathrm{K}$) can be estimated as $\sim S \times k_{\rm B}T/L^3 \simeq 4 \cdot 10^{-7}\,\mathrm{N}$. Even though these appear to be quite small forces, their magnitudes are actually comparable with the weight $\simeq 2 \cdot 10^{-7}\,\mathrm{N}$ of a water droplet of

account the expected proportionality to S, the two effects are characterized by different powers in their dependence on L.

[3] The scaling function $\Theta_\parallel$ actually depends also on whether a certain correlation length ξ is realized above or below the bulk critical temperature T_c. This is made clear later on by expressing the scaling function as a function of an appropriate scaling variable x, c.f., eq. (7), instead of $u = L/\xi$, as done here.

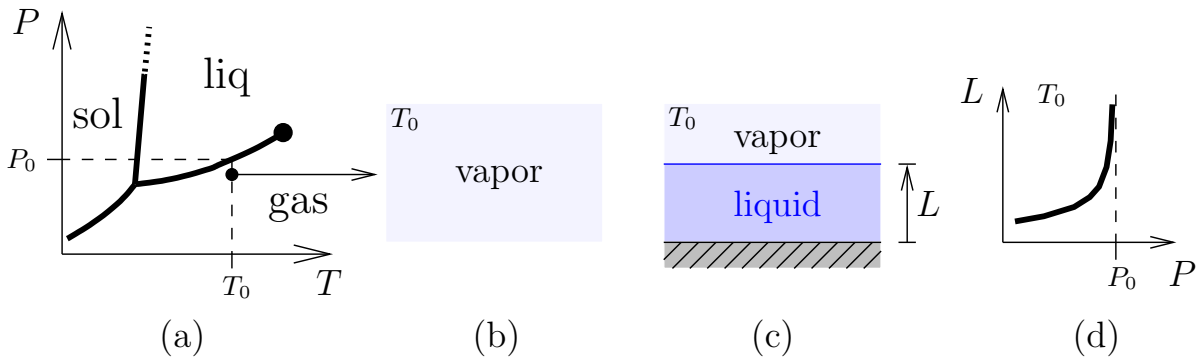

Figure 2. Formation of a *complete wetting* film of a fluid. Close to the liquid-gas phase transition (a), a vapor (b) condenses in the presence of a suitably chosen (solid) substrate, forming a liquid film (c), the thickness L of which diverges upon approaching the bulk condensation pressure P_0 (d).

half a millimeter in diameter. However, the realization of such a geometrical setting is actually extremely difficult due to the problem of maintaining the alignment between the two plates within the required accuracy. This problem is particularly difficult when trying to detect the Casimir effect in quantum electrodynamics and indeed this has been achieved in the parallel-plate geometry only quite recently [4]. For the detection of the critical Casimir effect the problem of alignment can be solved by taking advantage of physical phenomena, such as *wetting*, which naturally lead to the formation of confined films of fluids of a certain controllable and well-defined thickness L, determined by the thermodynamic parameters of the system, such as pressure and temperature [12, 13].

2.4. Wetting films and critical endpoints

In fig. 2(a) we depict schematically the phase diagram of a substance, as a function of the pressure P and temperature T, showing the generic solid (sol), liquid (liq), and gas phases. In order to obtain a liquid wetting film of this substance, the temperature T_0 and pressure P have to be chosen in such a way that the bulk system is in the vapor phase (fig. 2(b)) but close to the condensation transition, occurring at $P = P_0(T_0)$. If the vapor is taken in contact with a suitably chosen (solid) substrate (hatched grey area in fig. 2(c)), also at temperature T_0, a fluid film will condense on it as a consequence of the interaction of the substance with the substrate which makes the formation of a liquid layer thermodynamically favorable. The thickness L of the resulting film can be controlled acting on the undersaturation $\delta P = P - P_0(T_0)$ and is determined by van-der-Waals and dispersion forces. Depending on the choice of the substrate, L diverges smoothly upon approaching the bulk condensation pressure, i.e., for $\delta P \to 0$. This case is referred to as *complete wetting* and is characterized by the formation of a liquid film which can be made macroscopically thick, so that $L \gg \ell_{\rm micr}$. The phenomenon of wetting leads naturally to the formation of a liquid film of constant thickness L, in which the liquid is confined between the surface of the solid substrate and the liquid-vapor interface. The latter is macroscopically well defined sufficiently far from the liquid-vapor critical point. Even though the problem of the alignment between the confining surfaces is seemingly solved by wetting films, one has to be aware of the fact that the liquid-vapor interface actually fluctuates (*capillary fluctuations*) around its average position.

A possible *indirect* evidence of critical Casimir forces can be obtained by monitoring the thickness L of the wetting layer upon approaching a critical point which, in the bulk, occurs

within the liquid phase, is close to the liquid-vapor first-order transition but is far enough from the liquid-vapor critical point. This is the case for *critical endpoints* (cep), which are located where a line of critical points (within the liquid phase, see, c.f., fig. 3(a)) meets the liquid-vapor transition line. Indeed, upon approaching a critical endpoint, the critical fluctuations of the associated order parameter, confined within the liquid wetting film of thickness L, give rise to the critical Casimir effect. The associated force adds up to the previously acting (van-der-Waals) forces in determining the equilibrium distance L of the liquid-vapor interface from the substrate and consequently it affects the thickness of the wetting film. The dependence of L on the thermodynamic control parameters such as pressure and temperature is the basis for the determination of the Casimir force within this approach, which was proposed and discussed in detail in ref. [13] (see also ref. [14]) and provided the theoretical motivation for the experimental investigations summarized in subsec. 3.1.

3. The critical Casimir effect at work

In this section we summarize the theoretical predictions for the scaling function of the critical Casimir force in thin films and we compare them with the available experimental results based on wetting films (subsec. 3.1). Then we discuss a more direct measurement of this force (subsec. 3.2).

3.1. Wetting films

In subsec. 2.4 we argued that it is possible to exploit critical endpoints in order to infer the critical Casimir force from the thickness of a complete wetting film. One of the most studied fluids with such a critical endpoint is pure ^{4}He, the phase diagram of which is sketched in fig. 3(a). Within the fluid phase ^{4}He undergoes a second-order phase transition between a *sup*erfluid (also refereed to as HeII) and a *norm*al (HeI) behavior upon increasing the temperature across the so-called λ-line. The order parameter ϕ of this phase transition is physically provided by the wave-function of the superfluid. The λ-line terminates at the critical endpoint (cep) on the fluid-vapor first-order transition line (which ends on the right at the liquid-vapor critical point) located at low pressure, as indicated by the closer view of fig. 3(a). As previously described, in order to detect critical Casimir forces one prepares the system in the vapor phase corresponding to the point P in the closer view of fig. 3(a) and exposes this vapor to a suitable substrate (e.g., Cu) in order to obtain a complete wetting film of thickness L. Then one changes the thermodynamic parameters in such a way to follow the thermodynamic path indicated as γ in fig. 3(a), along which the film thickness L would not change in the absence of the critical endpoint. The actual changes are therefore due to the action of the critical Casimir force on the liquid-vapor interface and from these changes it is possible to determine experimentally the scaling function $\vartheta_{\|}$ of the force (see eq. (6)) [13]. In order to predict theoretically the scaling function $\vartheta_{\|}$ one has to single out a theoretical model which belongs to the same *bulk* and *surface* universality class as the confined ^{4}He. It is well known that the universal aspects of the bulk critical behavior of ^{4}He are properly captured, upon approaching the λ-line, by the lattice XY model [15], which lends itself, e.g., for Monte Carlo simulations. Accordingly, the behavior of a film of ^{4}He close to the λ-line is captured by the XY model with film geometry, where the boundary conditions on the lattice are chosen to be in the same surface universality class (i.e., to lead to the same effective boundary conditions for the order parameter) as the actual confining boundaries, represented by the substrate-liquid and liquid-vapor interfaces. As anticipated, the order parameter ϕ of the superfluid transition is related to the wave-function of the superfluid component and therefore, as a wave-function, it has to be continuous in space and to vanish both inside the substrate and within the vapor, where no superfluid is present. As a result, ϕ vanishes at the boundaries, i.e., ϕ satisfies Dirichlet BCs at both surfaces (DD). On the lattice model these BCs are realized via free boundary conditions for the degrees of freedom. Having identified a model which belongs to the same bulk and surface universality class as the film of

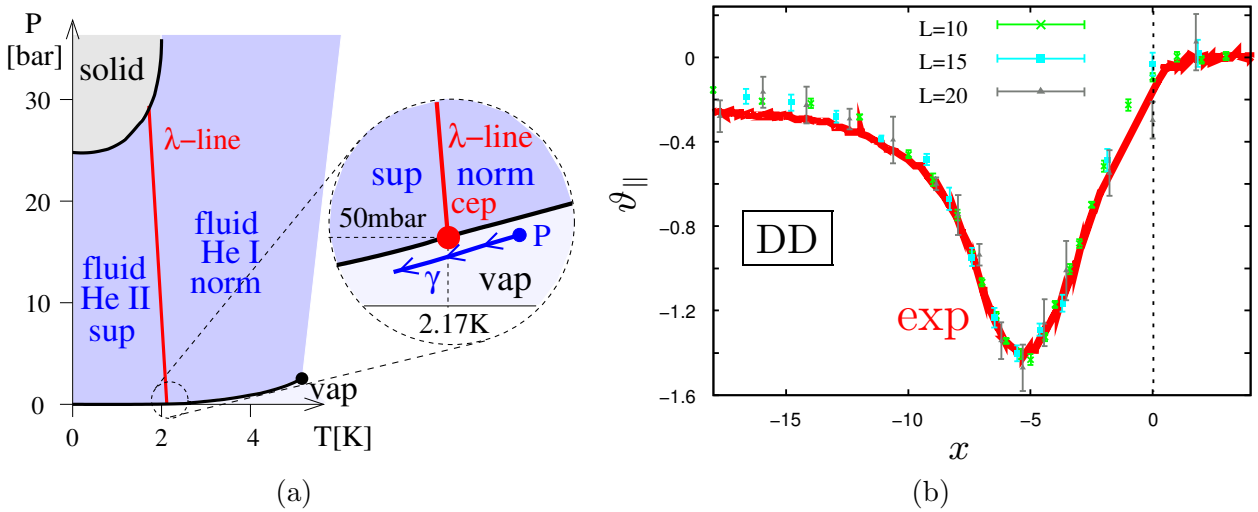

Figure 3. (a) Phase diagram of pure ^{4}He. The closer view highlights the presence of the critical endpoint (cep). (b) Universal scaling function $\vartheta_\parallel$ of the critical Casimir force within the three-dimensional XY universality class and Dirichlet-Dirichlet (DD) BCs, as a function of the scaling variable $x = (T/T_\lambda - 1)(L/\xi_0)^{1/\nu}$. The data points were obtained by Monte Carlo simulation of the XY model on the lattice in ref. [16], whereas the solid line represents the experimental results of ref. [20].

^{4}He, one can proceed to the determination of the scaling function $\vartheta_\parallel$. In fig. 3(b) the data points refer to the scaling function $\vartheta_\parallel$ as inferred from Monte Carlo simulations of the XY model in film geometry of various thicknesses and DD boundary conditions [16] (see also ref. [17]). The scaling function is plotted as a function of the proper scaling variable

$$x = t(L/\xi_0)^{1/\nu} \tag{7}$$

where $t \equiv (T - T_\lambda)/T_\lambda$, T is the temperature at which the lattice model is simulated and T_λ is the associated bulk critical value (corresponding to the λ-line in the actual system). L is the thickness of the film, ξ_0 the non-universal amplitude which controls the divergence of the bulk correlation length ξ and which can be determined independently via Monte Carlo simulation, and $\nu \simeq 0.66$ [15] is the universal critical exponent of the correlation length. The scaling variable x in eq. (7) is related to $u \equiv L/\xi$ in eq. (6) by $x = u^{1/\nu}$ for $t > 0$. As a confirmation of the scaling behavior in eq. (6), the scaling function $\vartheta_\parallel$ in fig. 3(b) does not depend on the thickness L of the film in which it has been numerically determined (as long as L is large enough compared to the lattice spacing) and the data sets corresponding to different sizes actually fall onto the same master curve. The predicted critical Casimir force turns out to be attractive in the whole range of temperatures ($\vartheta_\parallel < 0$), as expected it decays to zero for $L \gg \xi$, i.e., for $x \gg 1$, whereas it saturates to a non-vanishing value for $x \to -\infty$ due to the low-temperature long-range correlations maintained by Goldstone modes. Some of the qualitative features of the present force, such as the occurrence of a deep minimum below T_λ, can be understood within a simple mean-field approximation (see, e.g., refs. [18, 19]).

The very delicate experimental determination of the critical Casimir force acting on wetting films of ^{4}He on a Cu-substrate has been done in ref. [20], where the thickness $L \simeq 200 \ldots 300$ Å of the film as a function of the distance from the critical point has been determined by capacitance measurements. The corresponding experimental data are indicated by a solid line in fig. 3(b)

and show a remarkably good agreement with the corresponding theoretical predictions based on Monte Carlo simulations of the lattice model. In determining the value of the abscissa x corresponding to a certain experimental point one has to use for ξ_0 the system-specific value which has been determined independently in the experiment on the basis of the behavior of the bulk correlation length. If this is properly done, then there are no free parameters which can be adjusted in the comparison. In this sense the test of the theoretical predictions is remarkably stringent.

Based on the values of the experimental parameters of ref. [20] one can estimate the critical Casimir pressure to be of the order of 2 Pa which, however, is still of quite difficult detection in those experimental conditions. In order to increase the magnitude of the critical Casimir force, which is proportional to the temperature T, it is convenient to look for critical endpoints occurring at higher temperatures compared to the one of ^{4}He, for example by considering wetting films of *classical* binary liquid mixture. It turns out that in these cases the boundary conditions can be tuned such that the resulting forces are *repulsive*. These forces could find application for compensating the attractive electrodynamic Casimir force (the sign of which cannot be easily controlled) and therefore avoid stiction in micro- and nano-machines (MEMS and NEMS).

The phase diagram of a binary liquid mixture is depicted in fig. 1 for a fixed value of the pressure P (i.e., fig. 1 is a cut of the phase diagram in the (c_A, T, P)-space). Upon decreasing the pressure the location of the critical point CP changes in the (c_A, T)-plane and eventually it meets at the critical endpoint the sheet corresponding to the transition between the liquid and the vapor of the mixture. This critical endpoint can be exploited in order to create a wetting film of the binary mixture [13], similarly to the case of ^{4}He. The scaling function $\vartheta_{\|}$ can therefore be inferred by monitoring the equilibrium thickness of the wetting layer as a function of the thermodynamic parameters. Also in this case, theoretical predictions for the scaling function $\vartheta_{\|}$ can be obtained by studying a suitable model which belongs to the same *bulk* and *surface* universality class as the confined classical binary mixture. It is well-known that the bulk critical behavior close to the demixing critical point in a binary mixture is properly captured by the lattice Ising model [15], which lends itself, e.g., for numerical studies via Monte Carlo simulations. The universal behavior of the binary mixture confined in the film is therefore captured by the Ising model in a film geometry, in which the boundaries are chosen to be in the same surface universality class as the actual confining surfaces constituted by the substrate-liquid and liquid-vapor interfaces. In subsec. 2.2 we have already mentioned the fact that the boundaries generically show preferential adsorption for one of the two components of the mixture. As a result, the order parameter $\delta c_A(\mathbf{x})$ of the binary mixture (see the discussion in subsec. 2.2) either increases $(+)$ or decreases $(-)$ upon approaching the boundaries and this tendency turns into effective boundary conditions close enough to the critical point [8, 9]. We shall refer to the case in which both boundaries preferentially adsorb the *same* component of the mixture as $(++)$ and to the case of *opposite* preferences as $(+-)$. Additional details of the strength of this preferences etc. turn out to be irrelevant sufficiently close to the critical point. In the lattice Ising model, these boundary conditions are realized by fixing the lattice degrees of freedom (± 1 spins) on the two opposing boundaries either to the same $[(++)]$ or to opposite $[(+-)]$ values. The resulting numerical prediction of the scaling function $\vartheta_{\|}$ is reported in fig. 4 as a function of the scaling variable x in eq. (7), where L is the thickness of the film, $\nu \simeq 0.63$ [15] is the universal critical exponent of the correlation length, $t = (T - T_c)/T_c$ where T is the temperature at which the lattice model is simulated and T_c its critical value. As it was the case for ^{4}He, the value of the non-universal amplitude ξ_0 for this lattice model is measured independently via Monte Carlo simulations. The collapse of data points referring to lattices of different thicknesses onto the same master curve is again a confirmation of the scaling behavior expected on the basis of eq. (6)[4]. The sign of the resulting Casimir force depends on the boundary conditions and

[4] In order to extract in this case the asymptotic scaling behavior from Monte Carlo data it is necessary to account

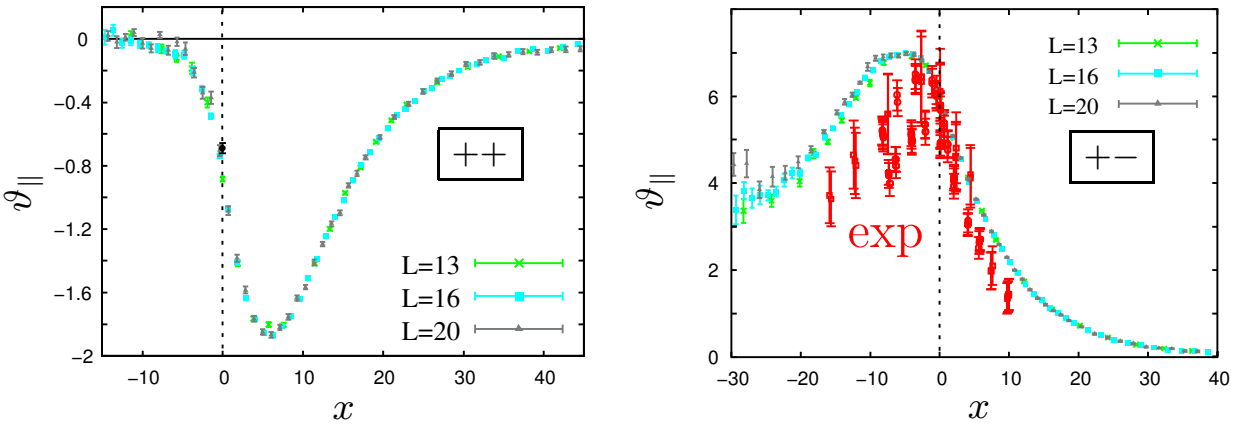

Figure 4. Universal scaling function $\vartheta_\parallel$ of the critical Casimir force within the three-dimensional Ising universality class and $(++)/(+-)$ BCs, as a function of the scaling variable $x = t(L/\xi_0)^{1/\nu}$. The data points were obtained in ref. [16] by Monte Carlo simulation of the Ising model on the lattice, whereas experimental data for the case of $(+-)$ BCs were obtained in ref. [22].

is *attractive* for $(++)$ and *repulsive* for $(+-)$, corresponding, respectively, to $\vartheta_\parallel(x) < 0$ and $\vartheta_\parallel(x) > 0$ in the whole range of temperatures. As expected, these scaling functions decay to zero for $x \to \pm\infty$ due to the fact that away from the critical point the correlation length becomes much smaller than the film thickness L both in the mixed (disordered in terms of the Ising model) and demixed (ordered) phase. In addition, the typical magnitude of the repulsive force for $(+-)$ BCs is larger than the one of the attractive force for $(++)$ boundary conditions. This is due to the fact that in the former case also the fluctuations of the position of the interface between the region with positive and negative values of $\langle \delta c_A(\mathbf{x}) \rangle$ contribute to the force acting on the confining surfaces. As in the case of ^{4}He some of the qualitative features of the force are already properly captured by a mean-field approximation [21]

The critical Casimir effect in wetting films of classical binary mixtures has been investigated in refs. [22, 23] where either ellipsometry [23] or X-ray scattering [22] techniques have been employed in order to determine the equilibrium thickness L of the wetting film. In particular in ref. [22] a binary mixture of methylcyclohexane (MC) and perfluoromethylcyclohexane (PFMC) has been used as the critical medium, with an upper critical point at temperature $T_c = 42.6°$C and molar fraction of PFMC $c_{\mathrm{PFMC},c} = 0.36$. The investigated wetting films were formed on a SiO_2/Si substrate and they had a typical thickness $L \simeq 100$ Å with the PFMC and MC preferring to be close to the liquid-vapor $(+)$ and the liquid-substrate $(-)$ interface, respectively. The corresponding experimental data for the inferred scaling function of the critical Casimir force are reported on the right panel of fig. 4. As in the comparison between theoretical and experimental predictions for ^{4}He, the value of the abscissa x corresponding to a certain experimental point has to be calculated according to eq. (7) taking into account the experimentally determined value of ξ_0 and the fact that $t \equiv (T - T_c)/T_c$ for an upper critical point. Note that, again, there are no adjustable parameters for the comparison. The agreement with the corresponding theoretical predictions is rather good (for a more detailed discussion, see ref. [16]).

All the evidence previously discussed for critical Casimir forces relies on the use of wetting films of (classical and quantum) fluids, a rather indirect way of detecting the effects of these

for corrections to scaling, see ref. [16] for details.

forces. In addition, the reliable quantitative interpretation of the observed variations of the thickness of these films in terms of the action of Casimir forces requires an independent and quite detailed knowledge of some material-dependent parameters which determine the van-der-Waals forces acting within the system. In view of these potential limitations, it would be desirable to measure *directly* the critical Casimir forces, e.g., by determining the associated potentials.

3.2. Brownian motion of colloids

The experimental evidence summarized in the previous subsection suggests that critical Casimir forces become relevant at the submicrometer scale, so that, on dimensional ground and for critical points at room temperature $T_c \simeq 300\,\mathrm{K}$ one estimates the typical scale of force as $\simeq k_\mathrm{B}T_c/(0.1\,\mu\mathrm{m}) \simeq 40\,\mathrm{fN}$. These tiny forces are hardly detectable even with very sensitive methods such as atomic force microscopy but nonetheless they are still strong enough to affect the Brownian motion of particles of micrometer size immersed in a fluid (i.e., *colloids*) which can be used as detectors. Indeed, under the effect of external forces (such as critical Casimir forces, gravity, buoyancy, etc., see below) a colloidal particle tends to stay at the equilibrium position $\mathbf{x}_\mathrm{eq}$ which corresponds to the minimum of the potential $\Phi(\mathbf{x})$ associated with the acting forces. However, due to the random collisions with the molecules of the surrounding fluid (in thermal equilibrium at temperature T), the particle actually fluctuates around $\mathbf{x}_\mathrm{eq}$, with a probability density $\rho(\mathbf{x}) \propto \exp\{-\Phi(\mathbf{x})/(k_\mathrm{B}T)\}$. Accordingly, the forces acting on a colloid can be inferred from the measurement of $\rho(\mathbf{x})$. This possibility suggests the study of a geometrical arrangement in which the critical fluctuations of the medium are restricted in the space between a spherical colloid and a planar surface rather than between two parallel surfaces, as considered so far. On the basis of the discussion of subsec. 2.2, one actually expects a Casimir force F to act on the sphere. If the minimal distance z between the surface of the sphere and the planar substrate is much smaller than the radius R of the sphere itself, the spherical surface can be approximated by a set of circular rings parallel to the opposing planar substrate (Derjaguin approximation) and therefore the force in this geometrical setting can be related to the one for parallel plates. Within this approximation, the z-dependent critical Casimir force F at temperature T acting on the sphere is given by (see ref. [25] for details)

$$F(z) = k_\mathrm{B}T\frac{R}{z^2}\vartheta_{|\circ}(z/\xi) \quad \text{for} \quad z \ll R, \tag{8}$$

where the universal scaling function $\vartheta_{|\circ}$ can be calculated in terms of a suitable integral of the scaling function $\vartheta_\parallel$ in a film [26] and it retains the qualitative features of $\vartheta_\parallel$. The theoretical prediction for the scaling form of the Casimir potential $\Phi_C(z) = \int_z^\infty \mathrm{d}z' F(z') = k_\mathrm{B}T(R/z)\Xi(z/\xi)$ immediately follows from the integration of eq. (8).

In order to measure tiny forces acting on a single colloid, one can take advantage of the Total Internal Reflection Microscopy (TIRM) [24], a very sensitive technique that is widely employed in the study of soft-matter systems [24]. With TIRM one monitors the Brownian motion of the colloid floating in a fluid and, as anticipated, from the associated statistics one infers the potential of the forces acting on the particle. The scheme of the experimental setup is depicted in fig. 5(a): an incoming visible laser beam is totally reflected at the substrate (glass)-fluid interface, so that an evanescent field of intensity $I_\mathrm{ev}(x_\perp)$ penetrates the liquid with a typical exponential decay as a function of the distance $x_\perp$ from the interface, see fig. 5(b). The colloidal particle, of suitable refractive index and at a surface-to-surface distance z from the substrate, scatters light out of this evanescent field. The intensity I_sc of the scattered light is measured by a photomultiplier (PM) and turns out to be proportional to the intensity $I_\mathrm{ev}(z)$ of the evanescent field. ¿From the time dependence of the scattered intensity $I_\mathrm{sc}(t) \propto I_\mathrm{ev}(z(t))$, represented in fig. 5(c), one can therefore calculate the time dependence of the particle-wall separation, i.e., $z(t)$. This dependence, depicted in fig. 5(d), reflects the Brownian motion of the particle under

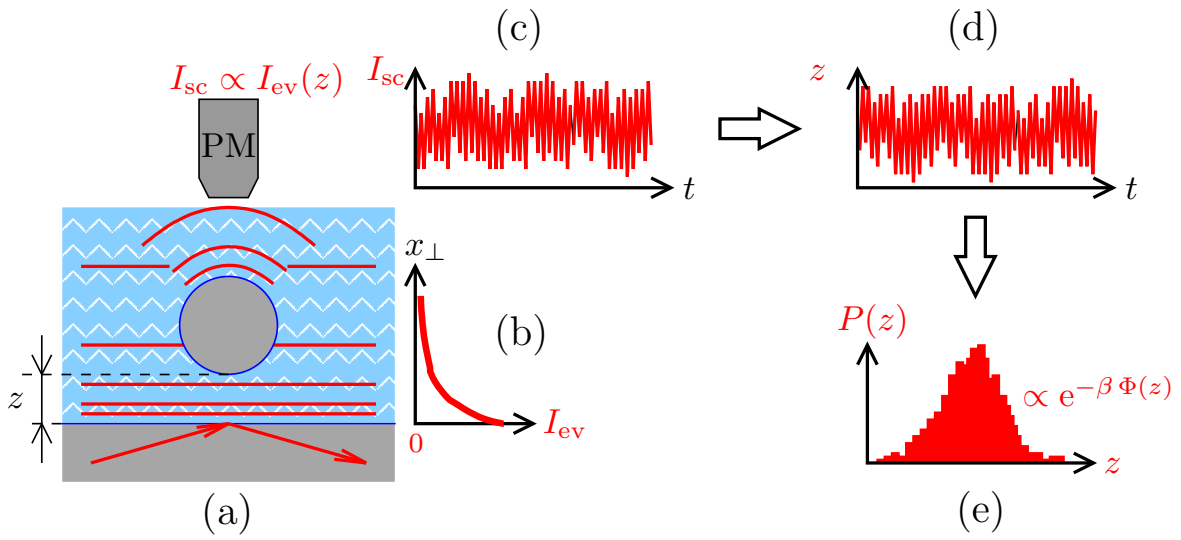

Figure 5. Determination of the potential $\Phi(z)$ of the forces acting on a single colloidal particle by means of the Total Internal Reflection Microscopy.

the effect of thermal fluctuations and possible additional forces. The probability distribution $P(z)$, as extracted from the histogram of $\{z(t)\}_{0\le t\le t_{\rm samp}}$ for sufficiently large sampling time $t_{\rm samp}$ (fig. 5(e)), is proportional to the Boltzmann factor $\exp\{-\beta\Phi(z)\}$ (with $\beta = (k_{\rm B}T)^{-1}$), where $\Phi(z)$ is the potential of the total force acting on the particle. Accordingly, $\Phi(z)$ can be calculated up to an irrelevant constant on the basis of the $P(z)$ inferred from the experimental data.

In order to provide a *direct* evidence of critical Casimir forces one can study a single colloidal particle immersed in a binary liquid mixture of water (W) and lutidine (L), close to a glass substrate [26]. In ref. [26] TIRM has been employed for the determination of the potential $\Phi(z)$ of the forces acting on the particle and for studying how Φ changes when the binary mixture is driven towards the critical point. The W-L mixture has a bulk phase diagram such as the one presented in fig. 1, with a lower critical point at $T_c = 34°$C and lutidine mass fraction $c_{{\rm L},c} \simeq 0.29$. The local excess concentration of lutidine $\delta c_{\rm L}(\mathbf{x})$ is a suitable order parameter for this demixing transition. In what follows we illustrate the experimental results in the case of a mixture at the critical concentration $c_{{\rm L},c}$ (the case $c_{\rm L} \neq c_{{\rm L},c}$ is discussed in refs. [25, 26]).

At a temperature T far below the critical value T_c, fluctuations of the order parameter are irrelevant and the potential $\Phi(z)$ of the forces acting on the particle is basically the sum of two contributions: (a) a screened electrostatic repulsion ($\Phi_{\rm el}(z) \propto e^{-\kappa z}$) between the colloid and the glass substrate, relevant in our experimental conditions for $z \lesssim 0.1\,\mu$m and (b) a linearly increasing potential due to the combined effect of buoyancy, gravity and optical pressures generated by the optical tweezer employed in the actual experimental setup[5]. This latter contribution has been subtracted from the curves presented in fig. 6, which show the dependence of the measured potential $\Phi(z)$ on the distance from the critical point. Panel (a) and (b) in fig. 6 refer to $(\text{colloid}, \text{substrate}) = (--)$ and $(+-)$ BCs, respectively. As expected, few hundreds mK far from the experimentally estimated critical temperature, the potential $\Phi(z)$ consists only of the electrostatic repulsion, which is negligible on this scale for $z \gtrsim 0.12\,\mu$m in (a) and $z \gtrsim 0.1\,\mu$m in (b). Upon increasing the temperature by few tens mK significant changes

[5] A third possible contribution, due to van-der-Waals forces turned out to be negligible in the experiment reported in refs. [26, 25].

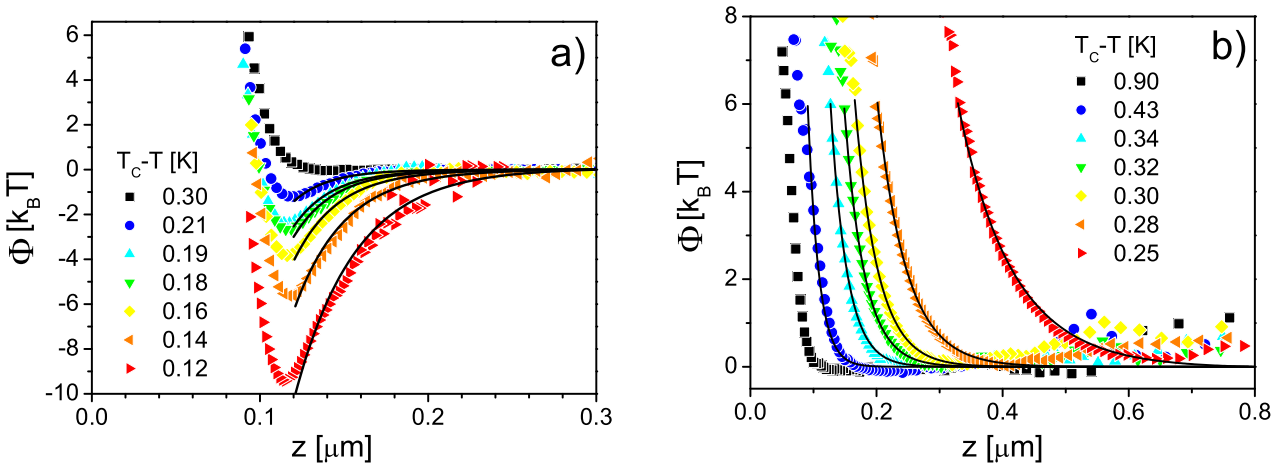

Figure 6. Temperature dependence of the potential $\Phi(z)$ of the forces acting on a single polystyrene colloidal particle at distance z of closest approach from a glass substrate. The particle and the substrate are immersed in a water-lutidine liquid mixture with critical composition and temperature T smaller than the critical one T_c. Data points refer to the experimental results (where gravity and buoyancy have been subtracted, see the main text) obtained for a substrate treated with NaOH in order to make it hydrophilic [$(-)$ BC for the order parameter] and (a) a colloid of diameter $2R = 2.4\,\mu$m absorbing preferentially water $(-)$ (b) a colloid of diameter $2R = 3.7\,\mu$m with preferential adsorption for lutidine $(+)$. The solid lines in (a) and (b) are the corresponding theoretical predictions for the critical Casimir potential with $(\text{colloid}, \text{substrate}) = (--)$ and $(+-)$ BCs, respectively. (From ref. [26].)

occur in the measured potentials: a strong attractive and repulsive force develops, respectively, in (a) and (b). In particular, in both cases one observes a change in the total potential of the order of 10 k_BT, which is really significant on the scale of k_BT which characterizes the physics of colloids. The maximum value of the attractive force acting in case (a) is estimated at 600 fN. The strong temperature dependence of the measured potentials is a clear indication of the involvement of critical Casimir forces. This evidence is supported by the comparison with the corresponding theoretical predictions for $\Phi_C(z)$, shown as solid lines in fig. 6. In order to focus only on the contribution to $\Phi(z)$ due to the critical Casimir force, this comparison is presented only within the range of distances where the electrostatic contribution is negligible. The limited accuracy with which the critical temperature T_c has been experimentally determined in ref. [26] does not allow a reliable calculation of the correlation length ξ on the basis of the theoretical relation $\xi = \xi_0(1 - T/T_c)^{-0.63}$ and of the value $\xi_0^{(\text{exp})}$ of ξ_0 measured for the W-L mixture in the bulk by independent experiments [27]. Instead, for each single temperature T, the correlation length $\xi(T)$ can be determined in order to optimize the agreement between theory and experimental data. Then, separately for the two experiments, the value $\xi_0^{(\text{fit})}$ of ξ_0 and $T_c^{(\text{fit})}$ of T_c are determined in such a way to yield the best fit of the determined $\xi(T)$ with the expected algebraic behavior. In both cases the fact that $\xi_0^{(\text{fit})} = \xi_0^{(\text{exp})}$ within errorbars is a check of the significant agreement between theory and experiments. (See refs. [25, 26] for a more detailed discussion.) Interestingly enough, via a suitable chemical surface treatment, it is possible to change quite easily the substrate from hydrophilic $(-)$ to hydrophobic $(+)$ and therefore switch the Casimir force acting on the colloids in fig. 6(a) and (b), respectively, from attractive to repulsive and vice-versa (see refs. [25, 26]).

Summing up, by measuring their effect on the Brownian motion of a colloidal particle, direct evidence of both attractive and repulsive critical Casimir forces has been provided. Based on the general arguments presented in subsec. 2.2 we expect such forces to act also between two or more colloids immersed in a near-critical mixture. Due to the strong non-additivity of these fluctuation-induced forces we expect interesting many-body effects.

4. Conclusions, perspectives and applications

4.1. Conclusions

In the previous sections we presented an overview of the Casimir effect due to critical fluctuations, highlighting its relation with the analogous effect in QED. We focused on the theoretical predictions which are relevant for the interpretation of the available and possibly forthcoming experiments, especially involving wetting films and colloidal particles. The comparison between the available theoretical and experimental results turns out to be very good. We did not attempt, however, to review of all the currently available relevant theoretical results and approaches, a task which is well beyond the scope of the present contribution. In what follows we mention only some of them.

The discussion in subsec. 2.2 clearly shows that Casimir-like effects are expected whenever the spectrum of fluctuations of a certain nature is changed by the presence of confining bodies, which consequently experience fluctuation-induced forces. The range of such forces is typically set by the correlation length ξ of the relevant fluctuations and a *universal* behavior has generally to be expected whenever $\xi, L \gg \ell_{\rm micr}$ where L is the typical distance between the boundaries and $\ell_{\rm micr}$ a microscopic, system-dependent scale.

4.2. Perspectives

In view of the quite general conditions under which such Casimir forces arise, several examples can be found in statistical physics. They occur not only at the critical points previously discussed, or in systems belonging to other bulk and surface universality classes (e.g., liquid crystals or complex fluids [7, 28]), but also close to *tric*ritical points. This instance has been studied both experimentally and theoretically [29, 18]. Due to the fact that the upper critical spatial dimensionality for a tricritical point is three, a mean-field approximation of suitable models captures rather well the features observed in experiments. Casimir-like forces result also from (long-ranged) fluctuations occurring in non-equilibrium steady states of different nature, from chemical reactions to granular matter, see, e.g., ref. [30], or from quantum fluctuations of the order parameter of a quantum phase transition [11]. However, at present, it is not clear how these predictions can be experimentally tested. On the other hand, there are experimentally relevant systems, such as Bose gases close to the Bose-Einstein condensation, which have not yet been studied with the aim of detecting critical Casimir forces, even though some quantitative theoretical predictions (see fig. 3(b)) are available beyond the case of ideal gases [31]. Thermal capillary fluctuations of the interface between two different liquids give rise to a Casimir force acting on two or more colloidal particles trapped at that interface [32]. In this case, the presence of the colloids alters the spectrum of these surface fluctuations, with the additional feature that the boundaries themselves at which the boundary conditions are imposed, represented by the contact line of the interface at the surface of the colloids, fluctuate (see ref. [32] for details). The resulting forces might be of relevance for understanding the topical problem of the interaction among colloids trapped at interfaces.

So far we have only considered homogeneous substrates and particles. However, in the presence of chemical or topographical modulations, such as the one depicted in fig. 7, novel phenomena are expected, including the emergence of lateral critical Casimir forces $F_{\|}$ and torques $\tau_{\rm Cas}$, still characterized by a universal scaling behavior. Some of the features of these forces have been studied in ref. [33] and might form the basis for the quantitative understanding of recent

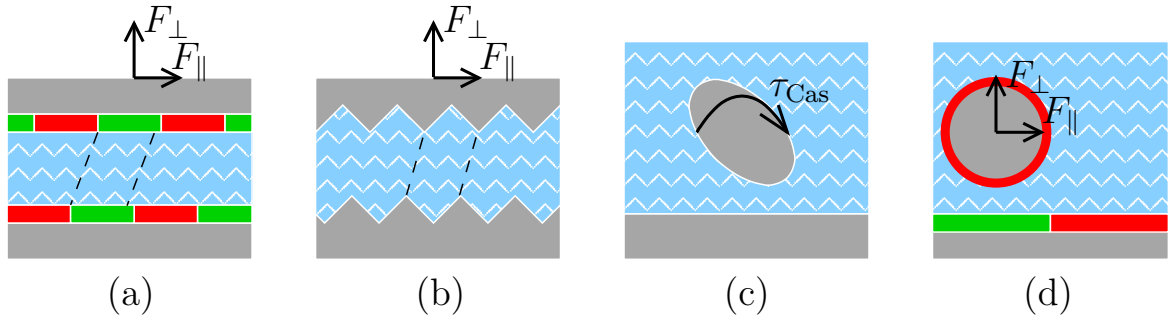

Figure 7. Possible chemically [(a), (d)] and topographically [(b)] patterned substrates in which a lateral critical Casimir force $F_\parallel$ arises in addition to the normal force $F_\perp$. A critical Casimir torque $\tau_{\rm Cas}$ is expected to act on non-spherical particles [(c)].

experimental investigation of the behavior of a single colloidal particle immersed in a binary mixture and exposed to a patterned substrate [34].

In addition to the equilibrium static behavior of the critical Casimir effect, its equilibrium and non-equilibrium dynamics pose both theoretical and experimental challenges. Indeed, it is not even obvious how to define theoretically such forces when their definition based on the decomposition of the effective free energy $\mathcal{F}$ (see eq. (5)) is no longer viable due to the lack of a proper notion of free energy for dynamical phenomena. A rich dynamical behavior is actually emerging already in quite simple theoretical relaxational models [35]. In order to make contact with the dynamical information which might come from TIRM experiments, it remains to be seen how the time-dependence of the critical Casimir force affects the Brownian motion of the colloidal particle in conjunction with hydrodynamic and adsorption phenomena.

4.3. Applications?

In contrast with the interactions typically acting among colloids (e.g., electrostatic), critical Casimir forces show a striking temperature dependence, as we have reported in subsec. 3.2. This fact can possibly be exploited in order to control via minute temperature changes the phase behavior and aggregation phenomena in systems with dispersed colloids. In addition, not only the range of interaction can be easily controlled but also the sign of the resulting force. This can be achieved by surface treatments and does not require (as it does for the quantum mechanical Casimir effect) substantial changes or tuning of the properties of the bulk materials which constitute the immersed objects. This property might be exploited in order to neutralize the attractive quantum mechanical Casimir force responsible for the stiction which brings micro-electromechanical systems to a standstill. If these machines would work not in a vacuum but in a liquid mixture close to the critical point, the stiction could be prevented by tuning the critical Casimir force to be repulsive via a suitable coating of the various machine parts. In principle, by using optically removable or controllable coatings, one could very conveniently control the functioning of the microdevice without acting directly on it.

Acknowledgments

I am grateful to C. Bechinger, S. Dietrich, L. Helden, C. Hertlein, A. Maciołek and O. Vasilyev for the stimulating collaborations which lead to some of the results summarized here and to M. Oettel and D. Dantchev for a careful reading of the manuscript.

References

[1] Casimir H B 1948 *Proc. K. Ned. Akad. Wet.* **51** 793

[2] Lamoreaux S K 1997 *Phys. Rev. Lett.* **78** 5
[3] Sparnaay M J 1958 *Physica* **24** 751
[4] Bressi G, Carugno G, Onofrio R and Ruoso G 2002 *Phys. Rev. Lett.* **88** 041804
[5] Lamoreaux S K 2007 *Physics Today* **60** 40
Ball P 2007 *Nature* **447** 772
Lambrecht A 2002 *Physics World* **15** 29
[6] Fisher M E and de Gennes P G 1978 *C. R. Acad. Sci. Paris Ser. B* **287** 207
[7] Kardar M and Golestanian R 1999 *Rev. Mod. Phys.* **71** 1233
[8] Binder K 1983 *Phase Transitions and Critical Phenomena* vol 8 eds C Domb and J L Lebowitz (London: Academic) p 1
[9] Diehl H W 1986 *Phase Transitions and Critical Phenomena* vol 10 eds C Domb and J L Lebowitz (London: Academic) p 76
[10] Krech M 1994 *Casimir Effect in Critical Systems* (Singapore: World Scientific)
1999 *J. Phys.: Condens. Matter* **11** R391
[11] Brankov G, Tonchev N S and Danchev D M 2000 *Theory of Critical Phenomena in Finite-Size Systems* (Singapore: World Scientific)
[12] Dietrich S 1988 *Phase Transitions and Critical Phenomena* vol 12 eds C Domb and J L Lebowitz (New York: Academic) p 1
[13] Krech M and Dietrich S 1992 *Phys. Rev. A* **46** 1922
[14] Nightingale M P and Indekeu J O 1985 *Phys. Rev. Lett.* **54** 1824
Indekeu J O 1986 *J. Chem. Soc. Faraday Trans. II* **82** 1835
[15] Pelissetto A and Vicari E 2002 *Phys. Rep.* **368** 549
[16] Vasilyev O, Gambassi A, Maciołek A and Dietrich S 2007 *EPL* **80** 60009
Preprint arXiv:0812.0750 (2008)
[17] Hucht A 2007 *Phys. Rev. Lett.* **99** 185301
[18] Maciołek A, Gambassi A and Dietrich S 2007 *Phys. Rev. E* **76** 031124
[19] Zandi R, Shackell A, Rudnick J, Kardar M and Chayes L P 2007 *Phys. Rev. E* **76** 030601(R)
Zandi R, Rudnick J and Kardar M 2004 *Phys. Rev. Lett.* **93** 155302
[20] Garcia R and Chan M H W 1999 *Phys. Rev. Lett.* **83** 1187
Ganshin A, Scheidemantel S, Garcia R and Chan M H W 2006 *Phys. Rev. Lett.* **97** 075301
[21] Krech M 1997 *Phys. Rev. E* **56** 1642
[22] Fukuto M, Yano Y F and Pershan P S 2005 *Phys. Rev. Lett.* **94** 135702
[23] Rafaï S, Bonn D and Meunier J 2007 *Physica A* **386** 31
[24] Prieve D C 1999 *Adv. Colloid Interf. Sci.* **82** 93
[25] Gambassi A, Maciołek A, Hertlein C, Nellen U, Helden L, Bechinger C and Dietrich S in preparation (2008)
[26] Hertlein C, Helden L, Gambassi A, Dietrich S and Bechinger C 2008 *Nature* **451** 172
[27] Gülari E, Collings A F, Schmidt R L and Pings C J 1972 *J. Chem. Phys.* **56** 6169
[28] Ziherl P, Podgornik R and Žumer S 1998 *Chem. Phys. Lett.* **295** 99
Bartolo D, Long D and Fournier J-B 2000 *Europhys. Lett.* **49** 729
Uchida N 2001 *Phys. Rev. Lett.* **87** 216101
[29] Krech M and Dietrich s 1992 *Phys. Rev. A* **46** 1886
Garcia R and Chan M H W 2002 *Phys. Rev. Lett.* **88** 086101
Maciołek A and Dietrich S 2006 *Europhys. Lett.* **74** 22
[30] Buenzli P R and Soto R 2008 *Phys. Rev. E* **78** 020102(R)
Buenzli P R contribution to this volume
Brito R, Soto R and Marini Bettolo Marconi U 2007 *Granular Matter* **10** 29
[31] Gambassi A and Dietrich S 2006 *Europhys. Lett.* **74** 754
Martin P A and Zagrebnov V A 2006 *Europhys. Lett.* **73** 15
[32] Lehle H, Oettel M and Dietrich S 2006 *Europhys. Lett.* **75** 174
Lehle H and Oettel M 2007 *Phys. Rev. E* **75** 011602
[33] Golestanian R, Ajdari A and Fournier J-B 2001 *Phys. Rev. E* **64** 022701
Karimi Pour Haddadan F, Schlesener F and Dietrich S 2004 *Phys. Rev. E* **70** 041701
Karimi Pour Haddadan F and Dietrich S 2006 *Phys. Rev. E* **73** 051708
Sprenger M, Schlesener F and Dietrich S 2006 *J. Chem. Phys.* **124** 134703
Tröndle M, Harnau L and Dietrich S 2008 *J. Chem. Phys.* **129** 124761
[34] Soyka F, Zvyagolskaya O, Hertlein C, Helden L and Bechinger C 2008 *Phys. Rev. Lett.* **101** 208301
[35] Gambassi A and Dietrich S 2006 *J. Stat. Phys.* **123** 929
Gambassi A 2008 *Eur. Phys. J. B* **64** 379